Physiological function and transplantation of scaffold-free and vascularized human cardiac muscle tissue

K. R. Stevens[a,b,c,d], K. L. Kreutziger[b,c,d], S. K. Dupras[b,c,d], F. S. Korte[a,d], M. Regnier[a,d], V. Muskheli[b,c,d], M. B. Nourse[b,c,d], K. Bendixen[b,c,d], H. Reinecke[b,c,d], and C. E. Murry[a,b,c,d,1]

Departments of [a]Bioengineering and [b]Pathology, [c]Center for Cardiovascular Biology, and [d]Institute for Stem Cell and Regenerative Medicine, University of Washington, Seattle, WA 98109

Communicated by William A. Catterall, University of Washington School of Medicine, Seattle, WA, August 11, 2009 (received for review February 19, 2009)

Success of human myocardial tissue engineering for cardiac repair has been limited by adverse effects of scaffold materials, necrosis at the tissue core, and poor survival after transplantation due to ischemic injury. Here, we report the development of scaffold-free prevascularized human heart tissue that survives in vivo transplantation and integrates with the host coronary circulation. Human embryonic stem cells (hESCs) were differentiated to cardiomyocytes by using activin A and BMP-4 and then placed into suspension on a rotating orbital shaker to create human cardiac tissue patches. Optimization of patch culture medium significantly increased cardiomyocyte viability in patch centers. These patches, composed only of enriched cardiomyocytes, did not survive to form significant grafts after implantation in vivo. To test the hypothesis that ischemic injury after transplantation would be attenuated by accelerated angiogenesis, we created ''second-generation,'' prevascularized, and entirely human patches from cardiomyocytes, endothelial cells (both human umbilical vein and hESC-derived endothelial cells), and fibroblasts. Functionally, vascularized patches actively contracted, could be electrically paced, and exhibited passive mechanics more similar to myocardium than patches comprising only cardiomyocytes. Implantation of these patches resulted in 10-fold larger cell grafts compared with patches composed only of cardiomyocytes. Moreover, the preformed human microvessels anastomosed with the rat host coronary circulation and delivered blood to the grafts. Thus, inclusion of vascular and stromal elements enhanced the in vitro performance of engineered human myocardium and markedly improved viability after transplantation. These studies demonstrate the importance of including vascular and stromal elements when designing human tissues for regenerative therapies.

angiogenesis | human embryonic stem cells | tissue engineering | myocardial infarction | cardiomyocyte

Stem cell-based reconstruction after myocardial infarction promises to restore function to the failing heart. New human myocardium has been formed recently in infarcted rodent hearts after injection of human embryonic stem cell (hESC)-derived cardiomyocytes, but small graft size and cell death currently limit the benefit of this therapy (1–3). Delivery of cells in tissue-like structures that preserve cellular attachments could increase cell delivery efficiency and reduce cell death (4). Most heart tissue engineered in vitro to date has focused on creating tissues by seeding neonatal rat or chick cardiomyocytes into polymer or extracellular matrix scaffolds and gels (5–11). Creation of 3D tissues that are composed only of cells and the matrix they secrete (12–15), which we refer to as "scaffold-free" tissue engineering, addresses limitations associated with polymer and exogenous matrix-based tissues (e.g., unfavorable host response to biomaterials). We recently created macroscopic scaffold-free human cardiac tissue constructs (16). These cardiac tissue patches were composed of highly enriched populations of human cardiomyocytes near patch edges, but like many other tissue engineered constructs (10, 17), they contained central necrosis due to the limitation of nutrient diffusion.

This study initially sought to optimize culture conditions to reduce the necrotic core and then test the ability of these first-generation human myocardial patches to engraft in vivo. Poor survival of these patches necessitated the addition of vascular endothelial cells and mesenchymal cells to create second-generation "prevascularized" patches. We show that second-generation patches actively contract, can be electrically paced, and have more myocardial-like passive mechanical properties compared with first-generation patches comprising only cardiomyocytes. Importantly, prevascularized patches show 10-fold greater survival after transplantation and form stable grafts of human myocardium and human blood vessels that anastomose to the host's coronary circulation.

Results

Media Optimization Reduces the Necrotic Core. We first sought to optimize culture conditions to minimize the necrotic core found previously in human cardiac tissue patches grown in human embryoid body (huEB) medium (16). Cellular necrosis at patch centers could be prevented by culturing patches in RPMI-B27 medium (*SI Text* and Fig. S1).

Patches Containing Only Cardiomyocytes Do Not Form Substantial Grafts in Vivo. To rapidly determine whether human cardiac tissue patches could engraft in muscle in vivo, we established a model of patch transplantation into skeletal muscle. Our previous work with direct injection of enzymatically dispersed cells demonstrated that death of cells during transplantation was multifactorial and that a "cocktail" of prosurvival interventions was required to achieve engraftment (1, 18). Patches containing 3×10^6 human cardiomyocytes cultured in the optimal RPMI-B27 media were therefore heat shocked 1 day before transplantation, bathed in prosurvival cocktail, and then implanted into the skeletal muscle of nude rats. At 1 week, the grafts consisted only of rare, isolated human cardiomyocytes, indicating that the vast majority of the engineered tissue had died, despite the use of prosurvival interventions that permitted the survival of cell suspensions. Further optimization of the cardiac tissue patches was clearly required.

Second-Generation, Vascularized Human Cardiac Tissue Patches. We reasoned that ischemia was contributing to cell death and that the

Author contributions: K.R.S., K.L.K., H.R., and C.E.M. designed research; K.R.S., K.L.K., S.K.D., F.S.K., V.M., and K.B. performed research; K.R.S., K.L.K., F.S.K., M.R., and M.B.N. contributed new reagents/analytic tools; K.R.S., K.L.K., and C.E.M. analyzed data; and K.R.S., K.L.K., H.R., and C.E.M. wrote the paper.

The authors declare no conflict of interest.

Freely available online through the PNAS open access option.

[1]To whom correspondence should be addressed. E-mail: murry@u.washington.edu.

This article contains supporting information online at www.pnas.org/cgi/content/full/0908381106/DCSupplemental.

thickness of the implanted patch was preventing diffusion-based survival before host angiogenesis could provide perfusion. We therefore sought to accelerate the process of vascularization by preforming vascular networks in the cardiac tissue patches. As a first attempt, we mixed human umbilical vein endothelial cells (HUVECs) with hESC-derived cardiomyocytes (cardio-HUVEC patches) in a 1:1 ratio during patch formation and then cultured patches in huEB media or RPMI-B27 for 8 days. The endothelial cells formed clusters of necrotic CD31-positive cells at the center of the patch, whereas cardiomyocytes remained viable at the periphery (3×10^6 cells of each type per patch; Fig. 1*A*). Several recent studies indicate that formation of vascular networks in tissue-engineered constructs is augmented by inclusion of mesenchymal cells that provide key paracrine factors and serve as supporting mural cells (9, 19, 20). We therefore constructed "tri-cell" cardiac patches containing hESC-derived cardiomyocytes, HUVECs, and mouse embryonic fibroblasts (MEFs) in 1:1:0.5 ratios, respectively (cardio-HUVEC-MEF patches). In sharp contrast to cardio-HUVEC patches, addition of MEFs to human cardiomyocytes and HUVECs resulted in the formation of human CD31-positive endothelial cell networks that morphologically resembled a vascular plexus (ratio 1:1:0.5 of cardiomyocytes to HUVECs to MEFs; 3×10^6 cardiomyocytes per patch; Fig. 1*A*). Patches comprising cardiomyocytes, HUVECs, and MEFs and cultured in huEB medium contained ≈20-fold more vessel structures than those comprising only cardiomyocytes or cardiomyocytes and HUVECs (Fig. 1*B*). The huEB medium tended to support the development of vessel-like structures slightly better than RPMI-B27 in all tri-cell experiments, and therefore we chose huEB medium as the standard culture media for cardio-HUVEC-MEF patches.

Similarly to HUVECs (Fig. 1*C*), creation of patches by using hESC-derived cardiomyocytes, hESC-derived endothelial cells, and MEFs (1.25×10^5, 1.25×10^5, and 0.625×10^5 cells, respectively) resulted in patches containing human CD31-positive structures that morphologically resembled blood vessels (Fig. 1*D*).

We hypothesized that paracrine factors secreted by the MEFs might be responsible for endothelial network morphogenesis. We cultured patches comprising only hESC-derived cardiomyocytes and HUVECs in MEF-conditioned huEB medium for 8 days. Endothelial networks did not form in these patches, suggesting that the stable paracrine signaling molecules secreted by MEFs were not sufficient to stimulate network formation.

Previous work suggested that the inclusion of MEFs in engineered cardiac tissue might also enhance cardiomyocyte proliferation (19). Cells in the S phase of the cell cycle were detected by using BrdU labeling in all patch types (Fig. S2*A*). The proliferation of human cardiomyocytes was enhanced by ≈50% in cardio-HUVEC-MEF patches compared with cardio-only and cardio-HUVEC patches ($P < 0.05$ for cardio-HUVEC patches vs. cardio-HUVEC-MEF patches; Fig. S2*B*).

In summary, these experiments demonstrate that proliferative human cardiac tissue patches containing endothelial cell networks morphologically resembling microvessels could be created by using human cardiomyocytes, HUVECs or hESC-derived endothelial cells, and fibroblasts, without the need for exogenous materials or matrices.

Patches Actively Contract in Response to Electrical Pacing. To test active contractile capacity and the ability of patches to be electrically paced, patches were field stimulated by using square waves of frequency (0.5–5 Hz), and contraction was monitored by using video edge detection (Fig. 2 *A* and *B*). Patches containing 2×10^6 cardiomyocytes (cardio-only) or 2×10^6 cardiomyocytes, 2×10^6 HUVECs, and 1×10^6 MEFs (cardio-HUVEC-MEF) were generated and cultured for 2–3 days in huEB medium before electrical pacing. Both cardio-only and cardio-HUVEC-MEF patches routinely followed stimuli greater or equal to 2 Hz (Fig. 2*C*). Patches showed reduced capacity to capture at 3-Hz stimulation, and no patches were able to keep pace to 5-Hz stimulation. Interestingly, pacing at higher frequencies prevented full relaxation of patches and a resultant decrease in contractile amplitude (e.g., as shown in 2-Hz frequency trace in Fig. 2*B*). In summary, human cardiac tissue patches actively contracted and could be electrically paced up to frequencies of 2–3 Hz.

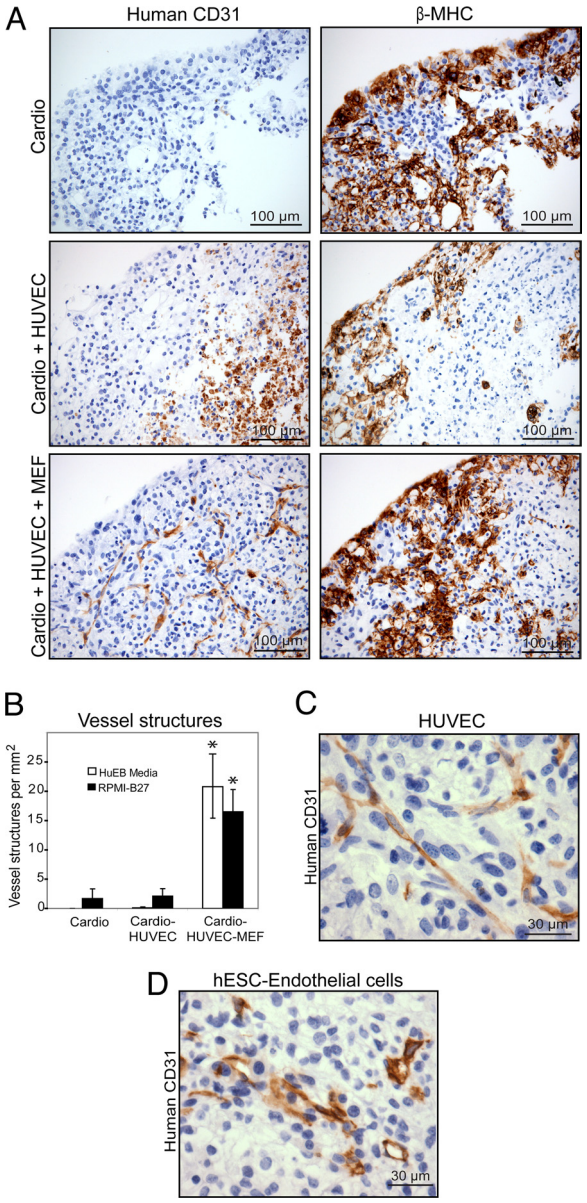

Fig. 1. Prevascularization of patches. (*A*) Representative images of patches created by using human cardiomyocytes, HUVECs, and/or MEFs cultured in huEB medium for 8 days are shown. Human endothelial cells stained for human CD31 (*Left*) and human cardiomyocytes stained for β-MHC (*Right*) are shown. Patches derived from cardiomyocytes only (*Top*) contained only rare CD31-positive cells. Patches derived from cardiomyocytes and HUVECs (*Middle*) were characterized by clumps of necrotic, CD31-positive debris, predominantly at the patch centers, and patches containing cardiomyocytes, HUVECs, and MEFs (*Bottom*) exhibited CD31-positive endothelial cell networks morphologically resembling a vascular plexus. (*B*) Patches comprising all three cell types contained significantly more vessel structures than patches comprising only cardiomyocytes or cardiomyocytes and HUVECs in both huEB and RPMI-B27 culture media. *, $P < 0.05$. Higher-magnification images of patches containing cardiomyocytes, HUVECs, and MEFs (*C*) or cardiomyocytes, hESC-derived endothelial cells, and MEFs (*D*) show that these patches contained human CD31-positive elongated vessel structures and lumens that morphologically resemble blood vessels.

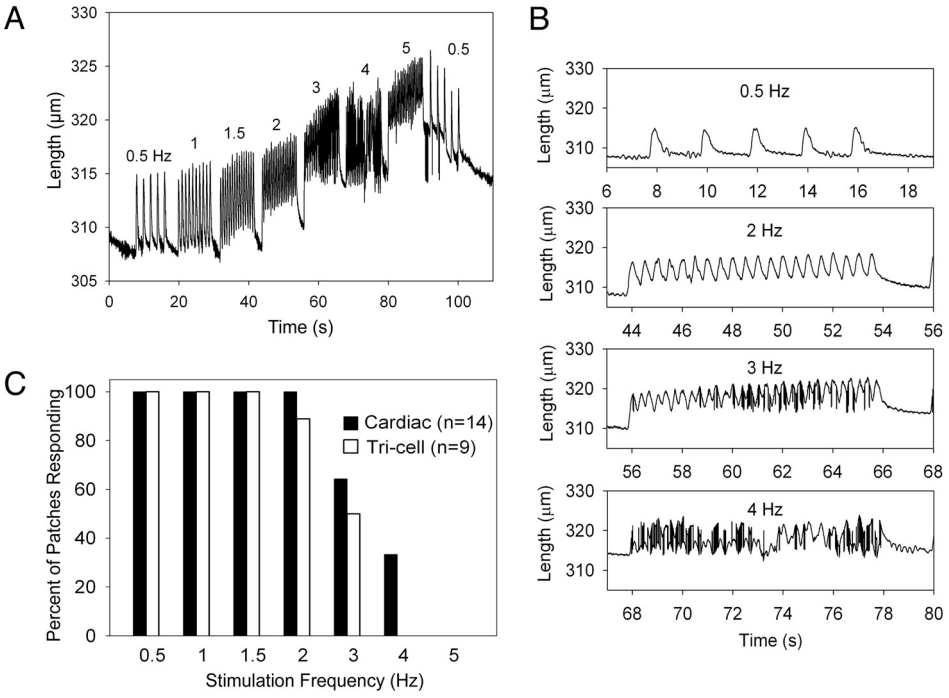

Fig. 2. Patches actively contract in response to electrical stimulation. Patches were electrically stimulated at frequencies of 0.5–5 Hz, and contraction was measured by using video edge detection. (*A*) A representative cardiomyocyte-only patch trace and (*B*) expanded views of select frequencies of this trace show a patch that captured 0.5- to 3-Hz but not 4- or 5-Hz stimuli. (*C*) Patches captured stimuli less than or equal to 2 Hz but exhibited reduced capacity to keep pace with frequencies of 3–5 Hz.

Enhanced Passive Mechanics in Cardio-HUVEC-MEF Patches. The passive mechanical properties of cardiac tissue play an important role in the mechanical function of the heart, particularly during diastolic filling. An ideal cardiac patch would have passive mechanical properties that resemble native myocardium. We measured the passive stiffness of cardio-only patches (2×10^6 cells per patch; cultured in huEB or RPMI-B27 media for 8 days) and cardio-HUVEC-MEF patches (2×10^6 cardiomyocytes, 2×10^6 HUVECs, and 1×10^6 MEFs per patch; cultured in huEB medium for 8 days) by using demembranated strips cut from patches. Patch strips were stretched in increasing-length increments with a square-wave protocol, and force was measured (Fig. 3*A*). Peak force was plotted as a function of the change in length and fitted with a line to determine the stiffness (Fig. 3*B*). Cardio-HUVEC-MEF patches had a stiffness of 7.9 ± 3.1 mN/mm^2 ($n = 5$ strips), which was approximately four times stiffer than cardio-only patches (stiffness of 2.0 ± 0.7 mN/mm^2; $n = 5$ strips; $P < 0.05$; Fig. 3*C*). By comparison, the stiffness of neonatal pig myocardium is 30.2 ± 3.5 mN/mm^2 (21). We hypothesized that the fibroblasts in the cardio-HUVEC-MEF constructs were producing connective tissue that altered passive stiffness. To test this, we stained patches with Sirius red (identifies collagen) and fast green (identifies other tissue elements). Cardio-HUVEC-MEF patches averaged more than 5-fold greater collagen per patch area and had more organized

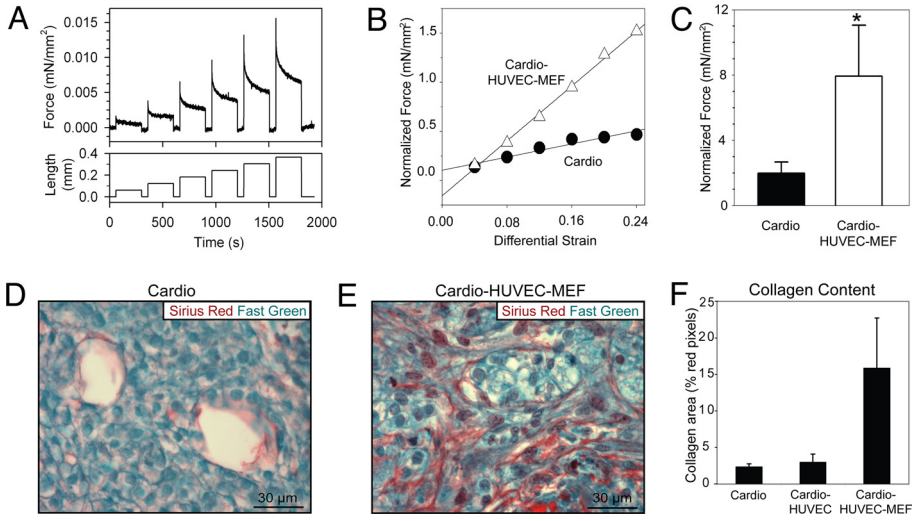

Fig. 3. Cardio-HUVEC-MEF patches are stiffer than patches composed of cardiomyocytes only. (*A*) Passive mechanical properties of patches were analyzed by stretching patch strips incrementally by using a square-wave length stretch protocol (*Lower*) and then measuring force (*Upper*). (*B*) Peak force elicited in response to increasing length increments for a representative cardio-HUVEC-MEF and cardio-only patch strip is shown. The slope of the force–strain line for a given patch strip denotes the stiffness of that strip. (*C*) The average stiffness of cardio-HUVEC-MEF patches was ≈4-fold greater than cardio-only patches. *, $P < 0.05$. (*D–F*) Patch sections were stained by using Sirius red (collagen) and fast green (other tissue elements). Representative cardio-only (*D*) and cardio-HUVEC-MEF (*E*) patches are shown. Cardio-HUVEC-MEF patches had greater than 5-fold collagen per unit area than cardio-only or cardio-HUVEC patches (*F*).

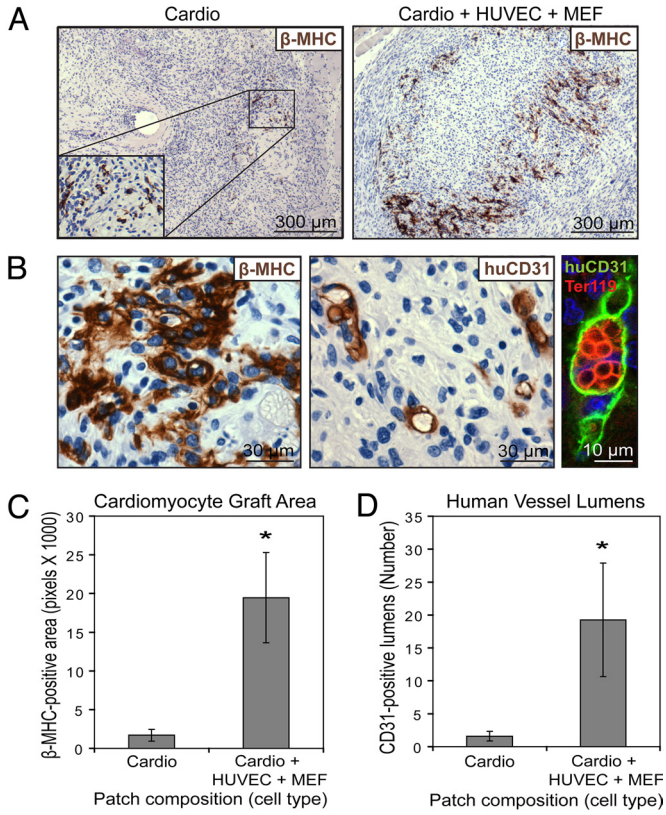

Fig. 4. Cardio-HUVEC-MEF patches form vascularized human grafts after implantation in skeletal muscle. Cardio-only or cardio-HUVEC-MEF patches were implanted in the gluteus superficialis muscle of nude rats for 1 week. Graft sections were immunostained by using antibodies against β-MHC, human CD31, and Ter-119 to identify human cardiomyocytes, human endothelial cells, and red blood cells, respectively. (*A*) Representative images of β-MHC-positive human cardiomyocyte grafts from animals implanted with patches comprising cardiomyocytes only (*Left inset* magnified 2×) or cardiomyocytes, HUVECs, and MEFs (*Right*). (*B*) Higher-magnification images of β-MHC-positive and human CD31-positive graft areas from a cardio-HUVEC-MEF patch implant showed that human cardiomyocytes remained small and structurally disorganized (*Left*) and that human CD31-positive cells formed vessel-like lumens containing Ter-119-positive red blood cells (*Middle* and *Right*). (*C*) β-MHC-positive cardiomyocyte graft area was ≈11-fold larger in animals that received cardio-HUVEC-MEF patches. *, $P < 0.05$. (*D*) Additionally, grafts in animals that received cardio-HUVEC-MEF patches had ≈12-fold more human CD31-positive vessel lumens than those that received cardio-only patches. *, $P < 0.05$.

collagen fibrils compared with cardio-only and cardio-HUVEC patches ($n = 3$ per group) (Fig. 3 *D–F*). Thus, cardio-HUVEC-MEF patches produced connective tissue and had more physiologically appropriate stiffness compared with cardio-only patches.

Cardio-HUVEC-MEF Patches Form Larger Grafts in Skeletal Muscle Model. We next sought to test whether prevascularization of human cardiac tissue patches would confer a survival advantage after implantation in vivo into skeletal muscle. Cardio-only or cardio-HUVEC-MEF patches containing 3×10^6 cardiomyocytes or 2×10^6 cardiomyocytes, 2×10^6 HUVECs, and 1×10^6 MEFs, respectively, were heat shocked and treated with our prosurvival cocktail before implantation into the gluteus muscle of nude rats. Rats were killed 1 week after patch implantation, and human cardiomyocytes and endothelial cells were identified by immunohistochemical staining for β-myosin heavy chain (β-MHC) and human CD31 (Fig. 4 *A* and *B*). As reported above, the cardio-only patches showed poor survival, with only occasional, isolated β-MHC-positive human cardiomyocytes detected. Rare microvessels containing human CD31-positive endothelium were noted. In contrast, the cardio-HUVEC-MEF patches formed much larger human myocardial grafts. Cardiac muscle cells in β-MHC-positive graft areas were small and exhibited immature sarcomeric organization, likely reflecting the early differentiation state of the cells (Fig. 4*B*). Numerous human CD31-positive endothelial cells were found in cardio-HUVEC-MEF patches, and many of these CD31-positive cells formed vessel-like lumens containing Ter-119-positive red blood cells (Fig. 4*B*). Importantly, histomorphometry revealed that the β-MHC-positive cardiomyocyte graft area was more than 11-fold larger in animals that received cardio-HUVEC-MEF patches than those that received cardio-only patches, despite the fact that cardio-only patches were generated with 50% more cardiomyocytes ($P < 0.05$; Fig. 4*C*). Additionally, grafts in animals that received cardio-HUVEC-MEF patches sections had ≈12-fold more human CD31-positive vessel lumens ($P < 0.05$; Fig. 4*D*). Thus, cardio-HUVEC-MEF patches formed significantly larger human cardiomyocyte grafts that contained more blood vessels than cardio-only patches in an in vivo muscle model. This indicates that the addition of HUVECs and MEFs imparted a survival and/or proliferative advantage to cardiomyocytes, and this survival was associated with the formation of perfused human microvessels in the patch implants.

Cardiac Tissue Patches Form Vascularized Human Myocardium in Rodent Hearts. To test whether cardio-HUVEC-MEF patches could form human myocardium in rodent hearts, these constructs were implanted onto nude rat hearts by using no additional attachment method beyond intrinsic tissue adhesiveness. One week after implantation, patches were found attached to the heart in two animals, wrapped in the pericardium (but dislodged from the heart) in two animals, and not found in two animals. To improve the attachment of patches to the hearts, cardio-HUVEC-MEF ($n = 4$) patches were sutured onto nude rat hearts. One week after implantation, all patches were found attached to the hearts (Fig. 5*A*). We next tested the engraftment of more clinically relevant patches composed entirely of human cells. Patches composed of human cardiomyocytes, HUVECs, and neonatal human dermal fibroblasts (cardio-HUVEC-NHDF patches; $n = 4$) were sutured onto nude rat hearts. Similarly to cardio-HUVEC-MEF patches, all patches were found attached to the hearts after 1 week.

Cardio-HUVEC-MEF and cardio-HUVEC-NHDF patch grafts contained significant β-MHC-positive and Nkx2.5-positive human myocardium and human CD31-positive endothelium. β-MHC-positive graft areas were closely apposed to the host myocardium but exhibited immature sarcomeric organization (Fig. 5 *B* and *C*). Many graft cells were Nkx2.5-positive but β-MHC-negative (Fig. 5*D*), suggesting that, similar to our previous in vitro findings (16), patches contained a significant population of cardiac progenitor cells that have not yet matured to express β-MHC. CD31-positive cells frequently formed vessel-like lumens that contained red blood cells and leukocytes, indicating that these vessels had anastomosed with the rat vasculature (Fig. 5 *E–G*). These results show that intracardiac implantation of prevascularized human cardiac tissue patches results in the formation of viable human myocardium and integrated human coronary microvessels.

Discussion

This study describes the in vitro optimization, functional characterization, and in vivo implantation of second-generation scaffold-free human cardiac tissue patches. In patches composed only of cardiomyocytes, optimization of cell culture media reduced central necrosis at patch centers. However, patches containing only cardiomyocytes exhibited poor survival after implantation in vivo. Second-generation prevascularized patches were therefore created by using human cardiomyocytes, endothelial cells, and fibroblasts. Functional characterization in vitro showed that these patches could actively contract, be electrically paced, and had more myo-

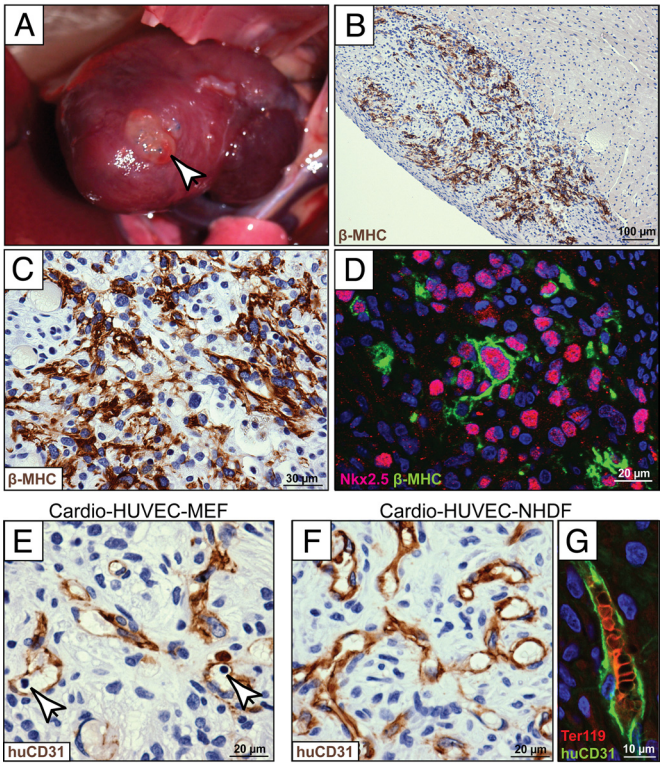

Fig. 5. Cardiac tissue patches form human cardiac muscle and integrated human microvessels in rodent hearts. Cardio-HUVEC-MEF or cardio-HUVEC-NHDF patches were implanted onto nude rat hearts for 1 week. (*A*) Gross examination of the heart immediately after sacrifice demonstrated that patches (arrow) attached with sutures were firmly adhered to the heart. (*B*) Patches had significant β-MHC-positive human cardiac muscle tissue (brown immunostaining; representative cardio-HUVEC-MEF patch). (*C*) A higher-magnification image of the graft from *B* shows that β-MHC-positive cardiomyocytes were relatively small and had immature sarcomeric organization, and that (*D*) grafts contained Nkx2.5-positive (pink nuclei) cardiac progenitor cells that had not yet matured to express β-MHC (green). CD31-positive endothelial cells in animals implanted with cardio-HUVEC-MEF (*E*) or cardio-HUVEC-NHDF (*F* and *G*) patches frequently formed vessel-like lumens that contained leukocytes (arrows in *E*) and Ter-119-positive red blood cells (*G*), indicating that grafted human vessels had connected with the host vasculature.

cardial-like passive mechanical stiffness compared with patches comprising only cardiomyocytes. Importantly, cardio-HUVEC-MEF patches formed greater than 10-fold larger human cardiomyocyte and endothelial cell grafts than cardiomyocyte-only patches after in vivo implantation in skeletal muscle. Cardio-HUVEC-MEF and entirely human cardio-HUVEC-NHDF patches also formed myocardium and microvessels after implantation onto rodent hearts.

We hypothesized that the first generation patches were dying from ischemic injury. We therefore aimed to create vascularized human cardiac tissue patches. In development, mesenchymal cells stabilize the maturation of young vessels, secreting paracrine pro-survival and proliferation signals and producing supportive extracellular matrix (22, 23). The addition of fibroblasts to cardiomyocytes and endothelial cells in patches resulted in the development of an endothelial cell network and enhanced cardiomyocyte proliferation. Importantly, we showed here that endothelial cell networks could also be created in scaffold-free patches by using clinically scalable hESC-derived endothelial cells. MEF-conditioned medium did not support the development of endothelial networks in patches comprising cardiomyocytes and HUVECs, suggesting that other signals, such as paracrine molecules not present in conditioned medium, direct cell–cell interactions, or the mesenchymal cell-derived matrix, are necessary for endothelial morphogenesis. Our results support recent findings in scaffold-based tissue engineering, in which fibroblasts synergized with endothelial cells in vessel formation and cardiomyocyte proliferation in vitro (9, 13, 19, 24). Our work details a previously undescribed scaffold-free approach to create vascularized human cardiac tissue.

The success of our scaffold-free patches to remuscularize the heart in vivo will require electrical synchrony with the host as well as mechanical contribution to systolic contraction and diastolic filling. We found that both cardio-only and cardio-HUVEC-MEF patches contracted in response to electrical stimuli up to at least 2 Hz (i.e., 120 beats per minute), suggesting that patches would be able to keep pace with adult human myocardium (typically ≈70 beats per minute). Further, the passive stiffness of cardio-HUVEC-MEF patches (≈8 mN/mm^2) was four times higher than cardio-only patches and was thus closer to that of neonatal pig and rat cardiac tissue (30.2 ± 3.5 mN/mm^2 in pigs, ref. 21; and 38.5 ± 9.1 mN/mm^2 in rats, ref. 25). Importantly, patches were ≈1,000 times less stiff than myocardial infarct scar (3730 ± 1340 mN/mm^2) (25), suggesting that they would not inhibit diastolic filling in vivo. The greater stiffness of the cardio-HUVEC-MEF patches is likely due to the ability of fibroblasts to secrete and rearrange extracellular matrix components in myocardium, as was evidenced by increased collagen found in cardio-HUVEC-MEF patches, although a direct role for fibroblast stiffness cannot be ruled out from these data. These results show that cardio-HUVEC-MEF patches are not only vascularized but also contain a connective tissue component.

The present study describes the in vivo engraftment of prevascularized engineered cardiac tissue composed entirely of human cells. Cardio-HUVEC-MEF patches resulted in greater than 10-fold larger β-MHC-positive (cardiomyocyte) and CD31-positive (endothelial cell) grafts than cardio-only grafts after implantation in a skeletal muscle model. Taken together with results from other groups in engineering skeletal muscle (20) and rat cardiac muscle (13), our results suggest a critical role for endothelial and mesenchymal cell populations in the design and implantation of engineered muscle tissue.

We showed here that prevascularized engineered cardiac tissue patches also form vascularized human myocardium after implantation onto rodent hearts. This suggests that human cardiomyocyte tissue patches could have broad clinical application in the repair of myocardial infarction and congenital heart defects. In the present study, we made significant progress toward clinical translation by creating entirely human cardiac tissue patches from hESC-derived cardiomyocytes, HUVECs, and NHDFs and demonstrating engraftment in animal hearts. Future studies will focus on testing alternative human cell sources (26, 27), developing techniques to create patches of appropriate size for epicardial treatment of large animals or for or injectable catheter-based delivery, and testing whether patches improve function after implantation on infarcted hearts.

Methods

Culture and Derivation of Cardiomyocytes and Endothelial Cells from hESCs. The undifferentiated female hESC H7 line (passages 58–96) was cultured in MEF-conditioned media, and hESC-derived cardiomyocytes and endothelial cells were derived by using directed differentiation protocols described previously (1) (see *SI Text* for additional details).

Creation of Patches Containing Cardiomyocytes, Endothelial Cells, and Fibroblasts. Human cardiomyocytes were removed from differentiation culture 18–26 days after the addition of activin A and then resuspended in huEB, RPMI-B27, or MEF-conditioned medium (see *SI Text* for additional details). HUVECs, hESC-derived endothelial cells, MEFs, and NHDFs were trypsinized and resuspended in corresponding media. We added 0.125×10^6 to 3×10^6 human cardiomyocytes, HUVECs, hESC-derived endothelial cells, MEFs, and/or NHDFs to low-attachment plates on day 0 in cardiomyocyte–endothelial cell–fibroblast ratios of 1:0:0, 1:1:0,

1:1:0.5, 1:1:1, 1:0.5:0.5, 1:0.5:0.25, or 1:2:0.5, with $n = 3–6$ per group. Plates were then placed on a rotating orbital shaker as described previously (16) and in *SI Text*.

Shortening Contractions Stimulated by Electrical Pacing in Whole Patches. Human cardiac tissue patches were paced with electrical field stimuli at frequencies of 0.5, 1, 1.5, 2, 3, 4, or 5 Hz (60 V; 25-ms square wave) by using an Aurora Scientific ($n = 14$ for cardio-only patches; $n = 9$ for cardio-HUVEC-MEF patches) stimulator (Model 700A) and a custom carbon electrode assembly fitted to a six-well tissue culture plate that was held at 30 °C ± 2 °C. Contractions were monitored and recorded digitally by using SoftEdge Acquisition software (IonOptix), which detects motion at a boundary or interface. Beating rate at each frequency was analyzed offline, and the number of patches that successfully captured all electrical impulses at a given frequency was recorded as a percentage of total patch number.

Passive Mechanical Measurements. Patches were cut into strips and passive tension response was measured by stretching patches in increments above initial length. Peak force from each length stretch was plotted versus fractional stretch and fitted with a line to obtain the stiffness of each patch strip preparation. The average stiffness of all preparations was determined for each patch type. See *SI Text* for additional details.

Preparation of Cardiac Tissue Patches for Implantation. To increase patch survival during the transplantation period, we adapted our recently developed prosurvival protocol (1) for use with engineered constructs, as detailed in the *SI Text*.

In Vivo Implantation into Skeletal Muscle. All animal procedures described were reviewed and approved by the University of Washington Institutional Animal Care and Use Committee and performed in accordance with federal guidelines for the care and use of laboratory animals. Sprague Dawley athymic nude rats (rnu-rnu; Charles River Laboratories) were anesthetized by using isofluorane. A small incision through the skin was made in the upper hindlimb, and fascia was trimmed for access to the gluteus superficialis muscle. Muscle fibers were parted by blunt dissection, and human cardiac tissue patches were inserted into the muscle. Two types of patches were implanted: (*i*) cardio-only patches contained 3×10^6 cardiomyocytes and were cultured in RPMI-B27 medium for 8 days before implantation ($n = 5$), and (*ii*) cardio-HUVEC-MEF patches contained 2×10^6 cardiomyocytes, 2×10^6 HUVECs, and 1×10^6 MEFs and were cultured in huEB medium for 8 days before implantation ($n = 4$). A 4-0 polyglycolic acid suture (Dexon-S, Syneture) was used to close the muscle and mark the location of patch placement. The incision in the skin was sutured closed, and the animal was allowed to recover. Animals were administered cyclosporine A s.c. 1 day before surgery and then daily until sacrifice (0.75 mg/day; Wako Pure Chemicals). Animals were killed 1 week after implantation. Skeletal muscle surrounding the site of patch implant was collected, sliced through the suture site with a razorblade, fixed in Methyl Carnoy's fixative (60% methanol, 30% chloroform, and 10% glacial acetic acid), processed, embedded, and sectioned into 5-μm sections for histology.

Patch Engraftment on Hearts. Sprague Dawley nude rats were anesthetized by using isofluorane, intubated, and mechanically ventilated. The chest was opened, the pericardium was partially removed from the heart, the heart was scuffed slightly with a cotton swab, and a single patch containing 2×10^6 cardiomyocytes, 2×10^6 HUVECs, and 1×10^6 MEFs or NHDFs cultured in huEB medium for 8 days was placed directly onto the heart (by using no additional attachment methods; $n = 6$ cardio-HUVEC-MEF patches) or attached to the heart by using two to four sutures ($n = 4$ for cardio-HUVEC-MEF patches; $n = 4$ for cardio-HUVEC-NHDF patches).

The chest was closed aseptically 15 min after application of patches, and animal recovery from surgery was monitored. Animals were administered cyclosporine A s.c. daily starting 1 day before and continuing for 7 days after patch implantation (0.75 mg/day; Wako Pure Chemicals). Animals were killed 1 week after patch implantation. Hearts were short-axis-sectioned through the patch, fixed in Methyl Carnoy's fixative, processed, embedded, and cut into 5-μm sections for histology.

Immunohistochemistry and Microscopy. For media optimization and proliferation experiments, patch sections were double-stained with antibodies against β-MHC and BrdU to identify cardiomyocytes and cells in the S phase of the cell cycle, respectively (16). For in vitro vascularization and in vivo implantation experiments, patch sections were stained with antibodies against β-MHC, Nkx2.5, human CD31, and Ter-119 to identify human cardiomyocytes, cardiac progenitor cells, endothelial cells, and red blood cells, respectively (16). See *SI Text* for additional information.

Note Added in Proof. We draw the reader's attention to two interesting articles, published while this manuscript was in the proof stage. Lesman et al. (28) transplanted prevascularized constructs containing hESC-derived cardiomyocytes, HUVECs, and MEFs and showed that they formed viable, perfused grafts in hearts of immunosuppressed rats. Dvir et al. (29) created a neonatal rat cardiomyocyte patch and prevascularized it on the omentum, prior to transplanting it onto the heart. They report these patches integrated structurally and electrically with the host heart. These reports support our finding that prevascularization enhances the ability of tissue engineered myocardium to engraft in the heart.

ACKNOWLEDGMENTS. We thank James Fugate, Mark Saiget, Nina Tan, Sarah Fernandes, and Jennifer Deem for expert technical assistance. This work was supported by National Institutes of Health Grants R01 HL64387, P01 HL03174, and R01 HL084642, U24 DK076126, and P01 GM081619; Bioengineering Cardiovascular Training Grant T32 EB001650-04 (to K.R.S.); and Experimental Pathology of Cardiovascular Disease Training Grant T32 HL07312-31 (to K.L.K.).

1. Laflamme MA, et al. (2007) Cardiomyocytes derived from human embryonic stem cells in pro-survival factors enhance function of infarcted rat hearts. *Nat Biotechnol* 25:1015–1024.
2. Caspi O, et al. (2007) Transplantation of human embryonic stem cell-derived cardiomyocytes improves myocardial performance in infarcted rat hearts. *J Am Coll Cardiol* 50:1884–1893.
3. van Laake LW, et al. (2007) Human embryonic stem cell-derived cardiomyocytes survive and mature in the mouse heart and transiently improve function after myocardial infarction. *Stem Cell Res* 1:9–24.
4. Simpson D, Liu H, Fan TH, Nerem R, Dudley SC, Jr (2007) A tissue engineering approach to progenitor cell delivery results in significant cell engraftment and improved myocardial remodeling. *Stem Cells* 25:2350–2357.
5. Carrier RL, et al. (1999) Cardiac tissue engineering: Cell seeding, cultivation parameters, and tissue construct characterization. *Biotechnol Bioeng* 64:580–589.
6. Eschenhagen T, et al. (1997) Three-dimensional reconstitution of embryonic cardiomyocytes in a collagen matrix: a new heart muscle model system. *FASEB J* 11:683–694.
7. Kutschka I, et al. (2006) Collagen matrices enhance survival of transplanted cardiomyoblasts and contribute to functional improvement of ischemic rat hearts. *Circulation* 114:I167–I173.
8. Li RK, et al. (1999) Survival and function of bioengineered cardiac grafts. *Circulation* 100:II63–II69.
9. Naito H, et al. (2006) Optimizing engineered heart tissue for therapeutic applications as surrogate heart muscle. *Circulation* 114:I72–I78.
10. Radisic M, et al. (2006) Biomimetic approach to cardiac tissue engineering: Oxygen carriers and channeled scaffolds. *Tissue Eng* 12:2077–2091.
11. Zimmermann WH, et al. (2006) Engineered heart tissue grafts improve systolic and diastolic function in infarcted rat hearts. *Nat Med* 12:452–458.
12. Moscona A, Moscona H (1952) The dissociation and aggregation of cells from organ rudiments of the early chick embryo. *J Anat* 86:287–301.
13. Sekine H, et al. (2008) Endothelial cell coculture within tissue-engineered cardiomyocyte sheets enhances neovascularization and improves cardiac function of ischemic hearts. *Circulation* 118:S145–S152.
14. Shimizu T, et al. (2006) Long-term survival and growth of pulsatile myocardial tissue grafts engineered by the layering of cardiomyocyte sheets. *Tissue Eng* 12:499–507.
15. Shimizu T, et al. (2002) Fabrication of pulsatile cardiac tissue grafts using a novel 3-dimensional cell sheet manipulation technique and temperature-responsive cell culture surfaces. *Circ Res* 90:e40.
16. Stevens KR, Pabon L, Muskheli V, Murry CE (2008) Scaffold-free human cardiac tissue patch created from embryonic stem cells. *Tissue Eng Part A* 15:1211–1222.
17. Eschenhagen T, Zimmermann WH (2005) Engineering myocardial tissue. *Circ Res* 97:1220–1231.
18. Robey TE, Saiget MK, Reinecke H, Murry CE (2008) Systems approaches to preventing transplanted cell death in cardiac repair. *J Mol Cell Cardiol* 45:567–581.
19. Caspi O, et al. (2007) Tissue engineering of vascularized cardiac muscle from human embryonic stem cells. *Circ Res* 100:263–272.
20. Levenberg S, et al. (2005) Engineering vascularized skeletal muscle tissue. *Nat Biotechnol* 23:879–884.
21. Lahmers S, Wu Y, Call DR, Labeit S, Granzier H (2004) Developmental control of titin isoform expression and passive stiffness in fetal and neonatal myocardium. *Circ Res* 94:505–513.
22. Koike N, et al. (2004) Tissue engineering: Creation of long-lasting blood vessels. *Nature* 428:138–139.
23. Loffredo F, Lee RT (2008) Therapeutic vasculogenesis: It takes two. *Circ Res* 103:128–130.
24. Chiu LL, Iyer RK, King JP, Radisic M (2008) Biphasic electrical field stimulation aids in tissue engineering of multicell-type cardiac organoids. *Tissue Eng Part A*, 10.1089/ten.tea.2007.0244.
25. Moreno-Gonzalez A, et al. (2009) Cell therapy enhances function of remote non-infarcted myocardium. *J Mol Cell Cardiol*, in press.
26. Park IH, et al. (2008) Reprogramming of human somatic cells to pluripotency with defined factors. *Nature* 451:141–146.
27. Yang L, et al. (2008) Human cardiovascular progenitor cells develop from a KDR+ embryonic-stem-cell-derived population. *Nature* 453:524–528.
28. Lesman A, et al. (2009) Transplantation of a tissue-engineered human vascularized cardiac muscle. *Tissue Eng Part A*, 10.1089/ten.TEA.2009.0130.
29. Dvir T, et al. (2009) Prevascularization of cardiac patch on the omentum improves its therapeutic outcome. *Proc Natl Acad Sci USA*, 10.1073/pnas.0812242106.

Supporting Information

Stevens et al. 10.1073/pnas.0908381106

SI Text

SI Methods. ***Culture and derivation of cardiomyocytes and endothelial cells from hESCs.*** The undifferentiated female hESC H7 line (passages 58–96) (1) was cultured in MEF-conditioned media consisting of 80% knockout DMEM (KO-DMEM; Invitrogen), 20% serum replacement, 1 mM L-glutamine (Gibco), 1% nonessential amino acids, 0.1 mM β-mercaptoethanol (Sigma), and 8 ng/ml basic FGF on tissue culture dishes coated with Matrigel (Growth Factor Reduced Matrigel; BD Biosciences) (2–5). Media were replaced daily on undifferentiated hESCs.

Cardiomyocytes were derived from hESCs by using the directed differentiation protocol described recently by Laflamme et al. (4). This protocol routinely yields greater than 30% cardiomyocytes (4). Briefly, undifferentiated hESCs were dispersed to single cells by using collagenase IV (200 units/ml; Gibco) and mechanical trituration and then were seeded onto Matrigel-coated plates at a density of 100,000 cells per square centimeter. When the cells became tightly packed (typically 3–5 days after plating), differentiation was induced by addition of activin A (50–100 ng/mL; R&D Systems) for 24 hours, followed by BMP-4 (10 ng/mL; R&D Systems) for 4 days in RPMI medium (Gibco) supplemented with 1× B27 supplement [RPMI-B27; B27 supplement includes L-carnitine HCl, recombinant human insulin, transferrin (human, iron-poor), sodium selenite, D-biotin, BSA, catalase, corticosterone, ethanolamine HCl, D-galactose, glutathione (reduced), linoleic acid, progesterone, putrescine-2HCl, superoxide dismutase, T-3–albumin complex, DL-alpha tocopherol, DL-alpha tocopherol acetate, and retinoic acid; Gibco]. Medium was then replaced 3 days per week with RPMI-B27 until beating foci, indicative of cardiomyocyte differentiation, appeared.

Endothelial cells were derived from hESCs by using the directed differentiation protocol described (6). Briefly, undifferentiated hESCs were dissociated into small clumps and placed in low-attachment plates in huEB (80% KO-DMEM, 1 mmol/L L-glutamine, 0.1 mmol/L β-mercaptoethanol, 1% nonessential amino acid stock, and 20% FBS; HyClone] containing 50 ng/mL VEGF (recombinant human vascular endothelial growth factor 165; donated generously by Genentech) to induce embryoid body formation and human endothelial cell differentiation. Embryoid bodies were plated onto 0.67% gelatin-coated plates after 4 days in suspension and then fed three times per week until day 14. Day-14 embryoid bodies were dispersed and stained with an antibody against CD31/PECAM-1 labeled with R-phycoerythrin (CD31-PE; BD Biosciences) for FACS. CD31-positive cells were collected by using a FACS Vantage cell sorter (BD Biosciences) and then expanded in endothelial growth media-2 (EGM-2; containing FBS, hydocortisone, human FGF, VEGF, human IGF-1, ascorbic acid, gentamicin-amphotericin-1000, and heparin; Lonza). Cells were used between three to seven passages after cell sorting.

Experiments for media and buffer optimization. Human cardiac tissue patches were created as described recently (7). Briefly, 14–18 days after the addition of activin A to hESC cultures, differentiated hESC-derived cells were enzymatically dispersed and resuspended in (*i*) huEB medium, (*ii*) supplemented M199 medium [M199 medium (Gibco), supplemented with 2 mM L-carnitine (Sigma), 5 mM creatine (Sigma), 5 mM taurine (Sigma), 1× insulin-transferrin-selenium-A supplement (Gibco), and 0.2% BSA (Sigma)], or (*iii*) RPMI-B27 medium with or without 20 mM Hepes buffer. hESC-derived cardiomyocytes were placed into each well of ultra-low-attachment six-well plates (Corning) at a concentration of 3×10^6 cells per well. Plates were placed on a rotating orbital shaker (1.9-cm orbital radius, 40 rpm; Barnstead) at 37 °C in a tissue culture incubator. The time at which cells were initially plated in suspension culture and placed on the rotating orbital shaker was referred to as day 0. Media were changed every other day. Patches were incubated with BrdU (10 μM; Roche) for 24 hours before fixation in methanol and 10% acetic acid on days 3 and 8 ($n = 5$ for each time point). Fixed patches were routinely processed and embedded in paraffin for histological examination.

Culture of HUVECs, mouse embryonic fibroblasts, and neonatal human dermal fibroblasts. HUVECs (Lonza) were cultured in EGM-2 on 0.67% gelatin-coated tissue culture plates. Cells were used between passages 4 and 9. Mouse embryonic fibroblasts (Chemicon) and NHDFs (Lonza) were cultured in fibroblast growth medium, consisting of DMEM (Gibco) supplemented with 10% FBS (HyClone), 2 mM L-glutamine, and penicillin/streptomycin (0.1 mg/mL; Gibco) on 0.67% gelatin-coated tissue culture plates. MEFs and NHDFs were used between passages 3 and 9.

MEF-conditioned medium experiments. HuEB medium was added to MEFs (70–100% confluent) for ≈24 hours. Conditioned media (1×) was collected, sterile-filtered, and added to patch culture on day 0. Media were changed once daily starting at day 2 and until the termination of the experiment on day 8.

Passive mechanical measurements. Patches were manually cut into ≈300-μm diameter × 1.3-mm-long strips. Patch strips were demembranated by using 1% Triton in 50:50 (vol/vol) glycerol/relaxing solution overnight and then transferred to glycerol/relaxing solution and stored at −20 °C for use within 1 week. Patch strip ends were chemically fixed with 1% glutaraldehyde in water and were wrapped in aluminum T clips for attachment to an Aurora Scientific force transducer and a General Scanning servomotor, as described previously (8). Initial patch strip length was set to 10% above slack length. Passive tension response was measured by stretching patches in increments of 4%, 8%, 12%, 16%, and 20% above initial length in relaxing solution [(pCa 9) 15 mM phosphocreatine, 15 mM EGTA, 80 mM MOPS, 1 mM free Mg^{2+}, 135 mM (Na^+ plus K^+), 5 mM ATP, and 1 mM DTT, pH 7.0, at 15 °C and ionic strength 0.17 M]. Each length stretch was followed by release of patch strips to initial length. Peak force from each length stretch was plotted versus fractional stretch (i.e., differential strain) and fitted with a line to obtain the stiffness of each patch strip preparation. The average stiffness of all preparations was determined for each patch type (e.g., patches containing only cardiomyocytes versus patches containing cardiomyocytes, endothelial cells, and fibroblasts).

Preparation of cardiac tissue patches for implantation. To increase patch survival during the transplantation period, we adapted our recently developed "prosurvival" protocol (4) for use with engineered constructs. Specifically, the day before in vivo implantation, patches were subjected to transient heat shock at 42 °C for 30 min. After heat shock, patches were returned to culture medium that was supplemented with IGF-1 (activates Akt pathways; 100 ng/mL; Peprotech) and cyclosporine A (attenuates cyclophilin D-dependent mitochondrial pathways; 2 μM; Wako Pure Chemicals) and cultured overnight. One hour before surgery, patches were placed in huEB medium supplemented with a prosurvival mixture (PSC) (1) containing ZVAD [caspase inhibitor; 10 μM, benzyloxycarbonyl-Val-Ala-Asp(*O*-methyl)-fluoromethyl ketone; Calbiochem], Bcl-X_L TAT-BH4 (blocks mitochondrial death pathways; 50 nM; Calbiochem), cyclosporine A (200 nM; Wako Pure Chemicals), IGF-1 (100

ng/mL; Peprotech), and pinacidil (K_{ATP}-channel opener; 50 μM; Sigma). Immediately before surgery, patches were washed twice in PBS containing PSC and then placed in PBS containing PSC (supplemented with 100 μM ZVAD) on ice until implantation.

Immunohistochemistry and microscopy. For analysis of in vitro patch histology, patches were fixed in methanol and 10% acetic acid and then paraffin-embedded for immunohistochemistry. Sections parallel to the patch's major surface area plane were cut from paraffin-embedded patch blocks. For media optimization and proliferation experiments, patch sections were double-stained with antibodies against β-MHC (clone A4.951; 1:10 dilution of hybridoma supernatant; American Type Culture Collection) to identify cardiomyocytes and BrdU (1:25; Roche) to identify cells in the S phase of the cell cycle as described previously (7). β-MHC antibody binding was visualized with the chromagen Vector Red (red staining; Vector Laboratories), and nuclear incorporation of BrdU was visualized with 1,3-diaminobenzidine (DAB; brown staining; Vector Laboratories). Sections were counterstained with hematoxylin. For media optimization studies in which the percentage of cardiomyocytes in patch centers was quantified, the numbers of β-MHC-positive and β-MHC-negative cells were counted in each of five randomly selected 40× fields that were more than 200 μm from the edge of each patch. For proliferation studies, BrdU and β-MHC double-positive nuclei were counted and recorded as a percentage of β-MHC-positive nuclei (percentage of proliferating cardiomyocytes), and BrdU-positive and β-MHC-negative nuclei were counted and recorded as a percentage of β-MHC-negative nuclei (percentage of proliferating noncardiomyocytes) in 10 randomly selected 40× fields of view in each patch. The numbers of β-MHC and/or BrdU positive and negative cells were used to determine the percentages of cardiomyocytes, proliferating cardiomyocytes, and proliferating noncardiomyocytes. Photographs of stained patch sections were obtained by using a light microscope (Nikon 80i) and QColor3 camera (Olympus).

For mechanics studies, patch sections were stained by using Sirius red and fast green to identify collagen fibers (red) and other tissue elements (green). Sections were rehydrated in a series of ethanol washes, stained in a solution of 0.1% Sirius red (Sigma) and 0.1% fast green (Sigma) in 1.3% picric acid (Sigma), and dehydrated in a series of ethanol washes. The number of red pixels in every patch was determined by using Photoshop (Adobe) for quantification of total collagen as a percentage of patch area.

For in vitro vascularization and in vivo implantation experiments, patch sections were stained with antibodies against β-MHC (clone A4.951; 1:10 dilution of hybridoma supernatant; American Type Culture Collection) and/or human CD31 (monoclonal mouse anti-human CD31; 1:20 dilution; Dako) to identify human cardiomyocytes and endothelial cells. Sections were blocked with 1.5% normal goat serum in PBS and then incubated with primary antibodies overnight at 4 °C. Sections were incubated with a goat secondary antibody raised against mouse (1:500 dilution; Jackson Laboratories) for 1 hour. Substrate-based staining was achieved by using the chromagen DAB. All slides were counterstained with hematoxylin to mark all cell nuclei. For in vitro vascularization studies, the total number of vessel-like structures (defined as elongated human CD31-positive cells that resembled vessels and were associated with a nucleus) were counted at 20× magnification and recorded as a ratio to total patch area. To measure β-MHC-positive graft size after implantation in skeletal muscle, total brown pixel area in each graft was determined by using Adobe Photoshop. Additionally, CD31-positive vessel lumens in each skeletal muscle graft section were counted at 20× magnification by using a Nikon 80i light microscope. For Nkx2.5 and β-MHC double staining, slides were incubated with an antibody against Nkx2.5 followed by a biotinylated horse anti-goat secondary antibody (Jackson Laboratories) and streptavidin Alexa 555 (Invitrogen). The β-MHC primary antibody was then followed by an Alexa 488-conjugated rabbit anti-mouse secondary antibody (Invitrogen), and counterstaining was performed with Hoechst 33342 nuclear dye (Sigma). To identify red blood cells in vessels containing human endothelial cells, patch sections were stained with antibodies against Ter-119 and human CD31. Sections were blocked with 1.5% normal goat serum in PBS and then incubated with the human CD31 antibody at 1:10 dilution overnight at 4 °C. Sections were incubated with a secondary goat anti-mouse Alexa 488 antibody (1:100 dilution; Invitrogen) for 1 hour at room temperature, washed in PBS, and then incubated with a PE-conjugated Ter-119 antibody (1:400 dilution; BD PharMingen) for 1 hour at room temperature. Slides were counterstained with DAPI (Vector Laboratories). Immunofluorescence images were obtained by using a confocal microscope (Zeiss LSM510 META).

Statistical analysis. Statistical significance ($P < 0.05$) was determined by using a one-tailed Student's t test assuming unequal variance for passive mechanics studies and a two-tailed Student's t test assuming unequal variance for all other studies. Error bars represent SEM.

SI Results and Discussion. ***Media optimization reduces the necrotic core.*** We originally sought to optimize culture conditions to minimize the necrotic core found previously in human cardiac tissue patches grown in huEB medium (containing 20% FBS) (7). Human cardiac tissue patches comprising only enriched hESC-derived cardiomyocytes were cultured in supplemented M199 medium, huEB medium, or RPMI-B27 medium (media commonly used for culturing rat neonatal cardiomyocytes, hESC-derived embryoid bodies, or hESC-derived cardiomyocytes for directed differentiation, respectively). Dramatic differences were observed between groups after 8 days of suspension culture. Patches cultured in supplemented M199 medium contained a necrotic core surrounded by a ring of viable cardiomyocytes (Fig. S1*A*). A similar pattern was found in patches cultured in huEB medium, but the border between viable cardiomyocytes and necrotic core was more gradual (Fig. S1*B*). Patches cultured in RPMI-B27 spontaneously segregated into two patches per well by 8 days of suspension culture in each of five wells. One of these patches contained a viable mixture of cardiomyocytes and nonmyocytes at the patch center (noncardiac RPMI-B27 patch; Fig. S1*C*). The other contained a highly pure population of cardiomyocytes (82% ± 8%) and substantially reduced necrosis throughout the patch center (Fig. S1*D*). The percentage of cardiomyocytes found in the center of the cardiac RPMI-B27 patches was significantly higher ($P < 0.05$) than those cultured in supplemented M199 or huEB medium ($P < 0.05$; Fig. S1*E*). Similar trends were found in two subsequent experiments, although RPMI-B27 patches sometimes did not separate into two distinct patches, but rather remained as one patch that had cellular composition intermediate between the noncardiac and cardiac RPMI-B27 patches. Cardiomyocyte proliferation (measured across patch edges and centers) was slightly reduced in cardiac RPMI-B27 patches compared with those cultured in supplemented M199 medium ($P < 0.05$; Fig. S1*F*). Noncardiomyocyte proliferation was significantly higher in the noncardiac RPMI-B27 patches compared with patches cultured in other media ($P < 0.01$; Fig. S1*G*). These results demonstrate that cellular necrosis at patch centers could be prevented by optimization of cell culture medium. These results could be due to the fact that the B27 supplement contains a variety of growth factors, antioxidants, steroids, and other compounds that may have served as an "antideath" mixture to spare the cells from necrosis. Alternatively, the reduced DNA synthesis in this group suggests that this medium may have reduced metabolic demand.

1. Thomson JA, et al. (1998) Embryonic stem cell lines derived from human blastocysts. *Science* 282:1145–1147.
2. Xu C, Police S, Rao N, Carpenter MK (2002) Characterization and enrichment of cardiomyocytes derived from human embryonic stem cells. *Circ Res* 91:501–508.
3. Laflamme MA, et al. (2005) Formation of human myocardium in the rat heart from human embryonic stem cells. *Am J Pathol* 167:663–671.
4. Laflamme MA, et al. (2007) Cardiomyocytes derived from human embryonic stem cells in pro-survival factors enhance function of infarcted rat hearts. *Nat Biotechnol* 25:1015–1024.
5. McDevitt TC, Laflamme MA, Murry CE (2005) Proliferation of cardiomyocytes derived from human embryonic stem cells is mediated via the IGF/PI 3-kinase/Akt signaling pathway. *J Mol Cell Cardiol* 39:865–873.
6. Nourse MB, et al. (2009) VEGF induces differentiation of endothelium from human embryonic stem cells: Implications for tissue engineering. *Arterioscler Thromb Vasc Biol*, in press.
7. Stevens KR, Pabon L, Muskheli V, Murry CE (2006) Scaffold-free human cardiac tissue patch created from embryonic stem cells. *Tissue Eng Part A* 15:1211–1222.
8. Kreutziger KL, Gillis TE, Davis JP, Tikunova SB, Regnier M (2007) Influence of enhanced troponin C Ca^{2+}-binding affinity on cooperative thin filament activation in rabbit skeletal muscle. *J Physiol* 58:337–350.

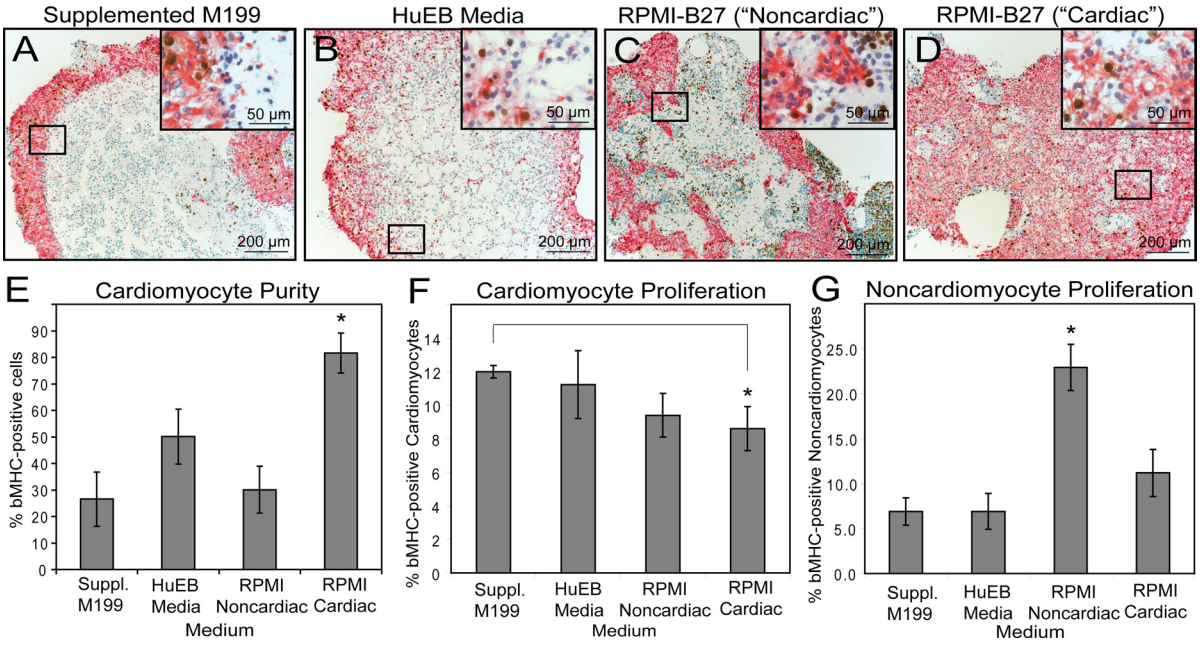

Fig. S1. Media optimization results in reduced central necrosis and increased cardiomyocyte purity. Representative images of patches cultured in supplemented M199 medium (*A*), huEB medium (*B*), or RPMI-B27 medium (*C* and *D*) and stained with antibodies against β-MHC (red cytoplasm; cardiomyocytes) and BrdU (brown nuclei; proliferating cells) show that the necrotic core in patches cultured in RPMI-B27 medium was largely replaced by viable cells, and in the case of cardiac RPMI-B27 patches, it was replaced by highly pure cardiomyocytes (*D*). (*E*) Cardiomyocyte purity at patch centers of cardiac RPMI-B27 patches was significantly higher than that for patches cultured in supplemented M199 or huEB medium. *, $P < 0.05$. (*F*) Cardiomyocyte proliferation at patch edges and centers was reduced in cardiac RPMI-B27 patches compared with those cultured in supplemented M199 medium. *, $P < 0.05$. (*G*) Proliferation of noncardiomyocytes was significantly higher in the noncardiac RPMI-B27 patches compared with patches cultured in other media. *, $P < 0.01$.

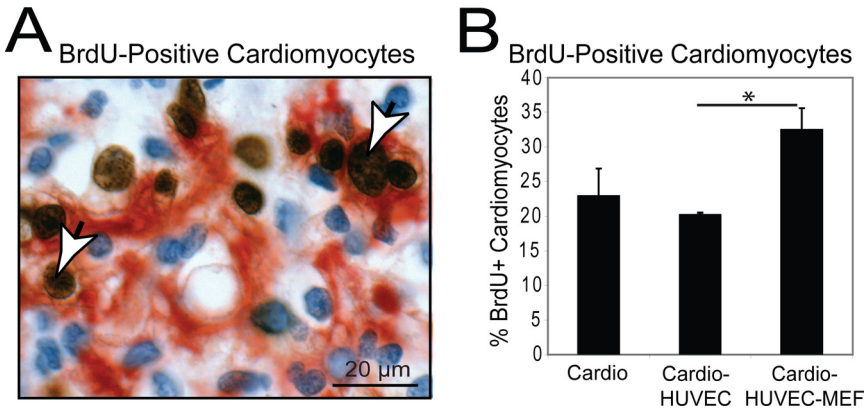

Fig. S2. Increased cardiomyocyte proliferation in tri-cell patches. Patch sections were double-stained for β-MHC (red cytoplasm; cardiomyocytes) and BrdU (brown nuclei; cells in S phase of cell cycle). (*A*) A representative image of proliferating cardiomyocytes (white arrows) in a patch containing cardiomyocytes, HUVECs, and MEFs is shown. (*B*) Human cardiomyocytes in patches comprising all three cell types exhibited enhanced proliferation compared with cardio-only or cardio-HUVEC patches. *, $P < 0.05$.